Current Eye Research
2000, Vol. 20, No. 4, pp. 293–312

0271-3683/00/2004-0293 $15.00

Quantitative analysis of the effect of near lens addition on accommodation and *myopigenesis*

George K. Hung[1] and Kenneth J. Ciuffreda[2]

[1]Department of Biomedical Engineering, Rutgers University, Piscataway, NJ, USA, and [2]Department of Vision Sciences, State College of Optometry, State University of New York, New York, USA

Abstract

Purpose. To develop a quantitative, objective, and scientific basis for understanding the effects of applying near bifocal additions (ADDs) on oculomotor control and myopia development. This is important because myopia is a major public health problem that affects 25% of the U.S. population and 75% or more in Asian countries. It is also associated with an increased risk for vision-threatening conditions, such as retinal breaks and detachments, as well as glaucoma.

Methods. A comprehensive model of refractive error development was constructed based on a dual-interactive feedback model of accommodation and vergence, which represented the short-term dynamics pathway, with the addition of both genetic and environmental (defocus-induced axial growth) components in a long-term pathway. An alternating near- and far-viewing paradigm was simulated, with varying amounts of ADDs, to obtain a parametric relationship between the root mean square of accommodative error (AE) and the induced refractive error (IRE). The parametric relationship provided the crucial linkage between the long-term growth pathway and the conventional short-term dynamics pathway. ADD is the simulated lens placed before the eyes only during near viewing, whereas IRE is the simulated lens fixed before the eyes that represents the optical effect of slowly progressive refractive development caused by near work.

Results. A V-shaped functional relationship was found between AE and IRE. The left half of the curve is associated with hyperopic defocus and myopigenesis, whereas the right half is associated with myopic defocus and hyperogenesis. Introduction of an ADD shifts the V-shaped curve horizontally. Thus, an "optimal" ADD can be used to shift the minimum of the accommodative error curve to the zero IRE point, and thereby reduce or eliminate retinal defocus and its potential towards myopigenesis. On the other hand, sensitivity analysis of model parameters shows that increasing the accommodative convergence crosslink gain (AC) shifts the curve to the right and results in a tendency towards myopigenesis, which is consistent with clinical findings in progressive myopia.

Conclusions. The model can be used to specify the precise ADD needed for an individual to retard or eliminate retinal defocus-induced myopic progression. If future experiments show that using the "optimal" ADD results in the greatest benefit (i.e., least myopia progression), there will be considerable worldwide public health benefit.

Keywords: refractive error development; emmetropization; myopia; near add; accommodation; control systems model; retinal defocus

Correspondence: George K. Hung, Department of Biomedical Engineering, Rutgers University, 617 Bowser Road, Piscataway, NJ 08854-8014, USA, Tel: (732) 445-4137, Fax: (732) 445-3753, E-mail: shoane@rci.rutgers.edu

Introduction

Myopia is an important public health problem worldwide.[1] It affects 25% of the adult population in the United States[2] and 75% or more of the adult population in Asian countries such as Taiwan.[3] Myopia is a refractive condition in which distant objects focus in front of the retina when accommodation is minimally stimulated. It can be corrected by optical means, but the estimated annualized cost to consumers in the United States for eye examinations and corrective lenses is $4.6 billion.[4] Furthermore, the wearing of spectacles for myopia may restrict one's vocational and avocational options.[5] Surgical techniques to reduce myopia are available but they are expensive, and despite the continual developments and technological improvements over the past 20 years, there are still surgical and post-surgical risks, along with possible side effects such as hazy vision.[4] Moreover, they do not prevent the subsequent development of adult-onset myopia or other age-related refractive changes.[4] Thus, myopia is a costly

Received on June 21, 1999; revised on December 12, 1999 and accepted on March 6, 2000

worldwide public health problem. For these reasons, the slowing of myopic progression, as well as the prevention of its initial occurrence, has been of considerable interest to clinicians and scientists alike for decades. Yet, a deeper understanding of the underlying potential myopigenic mechanisms has only recently begun to emerge.[6-22]

During the ocular growth and development phase of the human eye, if the cornea and lens grow perfectly in concert with the scleral tunic, there would be an exact match between the refractive (i.e., optical) and mechanical (i.e., ocular tunic) components of the eye, resulting in an absence of refractive error. However, a difference in their growth patterns, which results in a difference in their effective dioptric powers, will lead to a refractive error. It has been shown that both genetic and environmental[8,23-25] factors play important roles in refractive error development. For example, studies on twins have shown a high correlation in their refractive errors,[26-29] thus indicating a strong genetic component. On the other hand, population studies have shown a higher prevalence of myopia in those who engage in nearwork activity,[1,14,30-34] thus indicating a strong environmental component. Nearwork activity is associated with a larger lag of accommodation, or a greater amount of hyperopic defocus.[35]

Change in Retinal Defocus During Increment of Normal Genetically-Driven Axial Length Growth for Different Imposed Lenses.

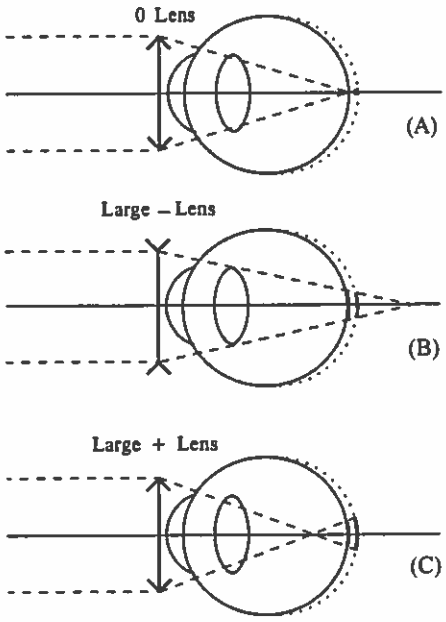

Figure 1. Schematic representation of change in blur circle during a small increment of normal genetically-driven ocular growth under the conditions of: (A) zero lens; (B) minus lens; and (C) plus lens. Adapted with permission from the authors.[49] (A) Below local blur threshold; Normal rate of neuromodulators; Normal growth rate. (B) Decrease in local blur magnitude; Decrease in rate of neuromodulators; Decrease in rate of proteoglycan synthesis; Increase in axial growth rate relative to normal. (C) Increase in local blur magnitude; Increase in rate of neuromodulators; Increase in rate of proteoglycan synthesis; Decrease in axial growth rate relative to normal.

If the hyperopic defocus is prolonged and sustained, it can result in an increase in the axial growth rate.[36] This produces a deviation from the optimal emmetropic growth pattern, with the consequent development of refractive error,[9,35,37-42] particularly late-onset myopia (see reviews by Ong and Ciuffreda[14,43]). Moreover, differences in individual susceptibility to nearwork effects add to the complex interplay between genetic and environmental factors in myopia development. For example, myopic children and young-adults are more susceptible to nearwork accommodative after-effects than either emmetropes or hyperopes.[35,44,45] Therefore, understanding the underlying mechanisms of myopia development and its prevention has been of considerable interest in recent years,[20,34] especially given the increased nearwork demands of children and young adults over the past few decades.[46-48]

Recently, a theory developed by us[49] proposed a mechanism to account for the animal study results, whereby the retinal signals associated with the change in blur magnitude during an increment of ocular growth can provide the signal for emmetropization (Figs. 1A-C). A schematic of the process is shown in Figs. 1 B,C for an initial (equal magnitude) hyperopic or myopic defocus, respectively. During an increment of normal genetically-driven axial length growth, the magnitude of retinal defocus will have decreased or increased, respectively (Figs. 1 B,C). It is proposed that feedback regulation provided by the interplexiform neurons from the inner to the outer plexiform layers, which aims to maintain a relatively constant sensitivity to retinal-mage contrast, leads to a decrease or increase, respectively, in neuromodulators such as dopamine. Such feedback regulation is useful because it would preclude the need for a memory mechanism for registering and storing previous levels of retinal defocus. The release of neuromodulators results in synaptic changes in the horizontal cells;[50,51] and this in turn alters the retinal sensitivity to center-surround input,[49] which helps to shift the steady-state operating level to permit responsivity to transient changes in local retinal-image contrast. The neuromodulators also cause structural changes in the sclera via modulation of proteoglycan synthesis[52,53] to result in correlated increase or decrease, respectively, in axial growth rate.[11,21,54-56] Thus, the differential change in defocus magnitude to imposed hyperopic or myopic defocus during an increment of normal ocular growth is proposed to provide the directional information needed to modify the rate of ocular growth to result in relative myopia or hyperopia (Fig. 1B,C), respectively

Yet, there remains one of the most profound and long-standing questions in oculomotor research, clinical vision care, public health epidemiology, and healthcare economics: *Can defocus-induced myopia progression be retarded or even eliminated, and can such reduction be precisely controlled?* An approach that has generated considerable interest is the use of near bifocal spectacle additions (ADDs) during the early stages of potential refractive error (RE) development.[57-61] The rationale for this approach is that the ADD reduces the net accommodative stimulus, and thus the ac-

commodative error, and its sensory equivalent, namely retinal defocus/blur. Since retinal defocus/blur has been implicated in the stimulation of axial length growth,[62-64] its reduction would inhibit axial elongation and the subsequent development of myopia.[42]

In addition, animal studies have shown that axial length growth rate can be altered with the imposition of large magnitude lenses.[13,18,56,65] Thus, with the imposition of large plus or minus lens, the eye becomes more hyperopic or myopic, respectively, relative to the normal-growing control eye. This refractive shift is highly correlated with changes in axial length.[13,18,56,65] Moreover, the stimulus for ocular growth occurs locally at the retinal level.[66]

Experimental studies up to this point have used a trial-and-error approach, with some investigators advocating low ADDs (< 1.50 D),[59,67-70] while other investigators advocating high ADDs (≥ 1.50 D)[60,61,71-76] (see Table 1). The results have been mixed. While some who used low ADDs found

Table 1. Effect of near bifocal ADD on myopia progression

	Near Bifocal ADD (D)	Age (yrs)	Number of Subjects	Mean or (Range) of Initial Myopia (D)	Rate of Progression (D/yr) (Significance of diff. between treatment and SV control)		
Goss (1986)	+0.75 to +1.50	6-15	SV: n = 52 BF: n = 60	(> 0.5)	Ortho or exo 0.44 0.45 (NS)	Eso 0.54 0.32 (p < .05)	
Schwartz (1980)	+1.25	7-13	SV: n = 25 BF: n = 25 (Twins)	2.22 2.33	0.27 0.24 (NS) Eso		
Fulk & Cyert (1996)	+1.25	M: 6-14 F: 6-13	SV: n = 14 BF: n = 14	2.10 2.20	0.57 0.39 (NS)		
Roberts & Banford (1967)	+0.75 to +2.00 (Most at +1.50)	Mean SV: 12.3 BF: 11.7	SV: n = 396 BF: n = 85	1.30 1.24	0.41 0.31 (p < .02)		
Grosvenor et al. (1987); Young et al. (1985)	+1.00 or +2.00	6-15	SV: n = 39 BF (+1D): n = 41 BF (+2D): n = 41	(> 0.25)	0.34 0.36 (NS) 0.34 (NS)		
Goss & Grosvenor (1990)	+1.00 or +2.00	6-15	SV: n = 32 BF: n = 65	Eso 1.89 2.16	Ortho or Exo 0.44 0.42 (NS)	Eso 0.51 0.31 (NS)	
Oakley & Young (1975)	+1.50 to +2.00	6-17	Nat. Am. SV: n = 83 192 BF: n = 43 226	White "Matched for initial refraction"	Native Am. 0.38 0.10 (p < .05)	White 0.53 0.02 (p < .001)	
Leung & Brown (1999)	+1.50 or +2.00	9-12	SV: n = 32 BF(+1D): n = 22 BF(+2D): n = 14	3.67 3.73 3.67	0.62 0.38 0.33	(p < .001) (p < .001)	
Parsinen et al. (1989)	+1.75	9-13	SV: n = 79 BF: n = 79	(0.25 to 3.00)	0.57 0.53 (NS)		
Jensen (1991)	+2.00	6-10	SV: n = 49 BF: n = 51	(1.25 to 6.00)	IOP ≤ 16 0.43 0.47 (NS)	IOP ≥ 17 0.66 0.49 (p < 0.38)	All 0.57 0.48 (NS)
Neetens and Evens (1985)	ADD varied with amount of develop. myopia: < 3D, plano; ≥ 3D, +2.50 ADD	8-9	SV: n = 733 BF: n = 543	(≤ 1 D)	0.45 0.30	(p < .001)	

less myopia progression than in the single-vision controls,[59,69] others who used high ADDs also reported reduction in myopia progression.[60,72,73,76] Yet, other investigators reported no improvement with either low[67,74,75] or high[61,74,75] ADDs. There has not been up to this time a complete and comprehensive model of refractive error development that can quantitatively specify the conditions for myopigenesis and hyperogenesis, in conjunction with a specific and traditional clinical lens therapy to retard or prevent myopia progression.

Such a comprehensive model is developed and analyzed in this study.[77] First, to investigate quantitatively the effect of bifocal ADD, accommodative convergence crosslink gain (AC), and convergence accommodation crosslink gain (CA) on retinal defocus, a static nonlinear model is developed and analyzed in detailed. Since the static model contains explicit equation solutions, it provides the foundation and quantitative basis for the subsequent dynamic analysis of the long-term effect of parameter variations on the nearwork model. Then, a dynamic refractive error development model that was constructed previously is used to simulate the effect of variation of bifocal ADD, as well as AC and CA, on the relationship between retinal defocus and refractive error.[77] Thus, the model provides a means to simulate various therapies (such as lenses) in different diagnostic groups (high AC/A, low AC/A, etc) to optimize the reduction of accommodative error. Finally, the model simulation findings provide a powerful clinical tool to prescribe precisely the individual near bifocal ADD for the reduction of myopia progression.

Material and methods

Static nonlinear model of accommodation and vergence

The complete static nonlinear model of accommodation and vergence (Fig. 2) is based on a previously developed static dual-interactive model of accommodation and vergence, which includes the nonlinear deadspace operators of depth-of-focus for accommodation and Panum's fusional area for vergence.[78,79] This model has been used successfully to simulate oculomotor conditions in amblyopia,[80] strabismus,[81] nearwork symptoms,[82,83] and myopia.[77] In addition to the basic model, the proximal contributions have been added[84] to account for the proximal effects found experimentally.[85] The complete static nonlinear model serves as the quantitative foundation for the understanding of parameter changes in the dynamic long-term nearwork model.[84] The derivation of the static nonlinear model equation for static accommodative error is given in the Appendix. Also, see the glossary in Table 2 for definition and expanded description of selected terms.

Static nonlinear model simulation

The equation for the static accommodative error of the complete static nonlinear model (Appendix – Eq. 18) was simulated using parameter values obtained previously[77,83,85] (see Table 3), for AS = 3 and VS = 3 MA. In addition to these fixed stimuli, a variable stimulus, called "induced" refractive error (IRE), was introduced (see Table 2). This was used to simulate the development of a small but uncorrected amount of new refractive change, as might occur between vision examinations, and is similar to placing a lens in front of the subject's eye. However, IRE should be distinguished from the subject's initial refractive condition per se (i.e., hyperopia (HYP), emmetropia (EMM), early-onset myopia (EOM) and late-onset myopia (LOM)), which is represented by internal parameter values in the model (see Table 3), and is optically corrected during the simulations. All the static simulation data were plotted in the form of AE vs. IRE, with IRE ranging from –3.0 to 3.0 D. Also, a sensitivity analysis was performed for AC and CA at 50, 100, and 150% of their nominal values (0.80 and 0.37, respectively). For example, first, at 100% of their nominal values, or 0.80 and 0.37, respectively, a model simulation was performed and a curve was obtained. Then, with the other parameters unchanged, AC was changed to 50% of its nominal value, or 0.40, and a second simulation was performed. Further, AC was then changed to 150% of its nominal value, or 1.20, and a third simulation was performed. The resulting three curves could then be compared to provide a graphical representation of the sensitivity of the model output to variations in AC. This procedure was repeated for CA. Following the sensitivity analysis, a static schematic analysis of directional selectivity of retinal defocus for an increment of IRE was performed for ADD = –2 and +2 D.

B. Dynamic models

Dynamic Adaptation Model of accommodation and vergence – configuration

The Dynamic Adaptation Model was based on a previously-developed static dual-interactive model of accommodation and vergence,[78] and is described in detail elsewhere.[83] It consisted of two feedback control loops driven by target defocus and binocular disparity, respectively (Fig. 3). The two loops were connected via the accommodative convergence (AC) and convergence accommodation (CA) crosslinks. In the accommodative loop, the difference between the accommodative stimulus (AS) and response (AR), or accommodative error (AE) (i.e., retinal defocus), was input to the nonlinear deadspace element (± AD), representing the depth-of-focus. If this input exceeded the depth-of-focus, then the output, which was now the retinal image blur, was input to the accommodative controller having gain ACG. The accommodative controller output was summed with tonic accommodation (ABIAS), and the crosslink signal via convergence accommodation to provide the aggregate accommodative response. Also, the accommodative output controller was multiplied by the crosslink gain, AC, to provide the accommodative convergence signal. For the vergence system, there is an analogous set of elements.

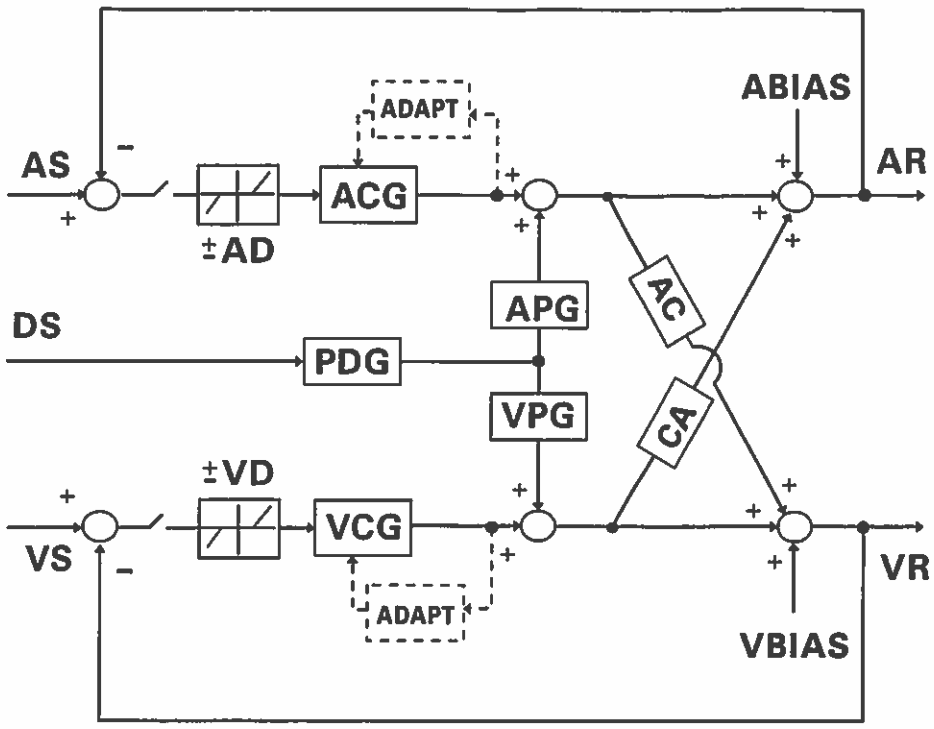

Figure 2. Complete nonlinear static interactive dual-feedback model of the accommodative and vergence systems. For the *accommodative* system, the switch controls feedback to accommodation. With the switch open, the input to the accommodative deadspace operator (± AD, which represents the depth-of-focus) is zero. On the other hand, with the switch closed, defocus blur, or the difference between accommodative stimulus (AS) and accommodative response AR, i.e., accommodative error, is input to accommodative deadspace operator. The output is multiplied with the accommodative controller gain, ACG, to give the accommodative controller output. The controller output is input to an adaptive element (ADAPT), which in turn controls the time constant of the accommodative controller. The distance stimulus (DS), or the distance of the target from the viewing subject, is input to the perceived distance gain (PDG) element, which represents the subjective apparent distance estimate. The PDG output then goes through the accommodative proximal gain (APG) element, which represents the contribution from target proximity. The outputs from ACG and APG are summed at the summing junction and are also cross-linked to the vergence system via gain AC. The accommodative bias (ABIAS), or tonic accommodation, is also summed at the summing junction along with the cross-link signal from the vergence controller output via CA. These four signals are added together to give the overall accommodative response, AR. For the *vergence* system, the switch controls feedback to vergence. With the switch open, the input to the vergence deadspace operator (± VD, which represents Panum's fusional area), is zero. On the other hand, with the switch closed, fixation disparity, or the difference between the vergence stimulus (VS) and vergence response (VR), i.e., vergence error, is input to the vergence deadspace operator. The output is multiplied with vergence controller gain, VCG, to give the vergence controller output. The controller output is input to an adaptive element (ADAPT), which in turn controls the time constant of the vergence controller. The distance stimulus (DS) is input to the perceived distance gain (PDG) element, which represents the subjective apparent distance estimate. It then goes through the vergence proximal gain (VPG) element, which represents the contribution from target proximity. The outputs of VCG and VPG are summed at the summing junction and are also cross-linked to the accommodation system via gain CA. The vergence bias (VBIAS), or tonic vergence, is also summed at the summing junction along with the cross-link signal from the accommodative controller output via AC. These four signals are added together to give the overall vergence system output, VR. The elements shown by dashed lines (ADAPT) are not used in the static model simulation. (Adapted with permission from Hung *et al.*[84])

In addition to the basic dual-interactive model, the unique feature of this model was the incorporation of both adaptive[82] and proximal[84] elements. The adaptive element in each loop received its input signal from the controller output, which in turn modified the time constant of the controller itself. For example, the accommodative controller output was input to a multiplier, m_A, and compression element, CE, to drive the adaptive element having gain, K_A, and time constant, T_{A1}. The multiplier and compression elements were necessary to provide a saturation effect for large inputs that was seen in the adaptation experiments.[86,87] The adaptive element output, a, modified the time constant of the accommodative controller via the term, $T_{A2} + |a^3|$, where T_{A2} was the fixed portion of the time constant. The cubic relationship was obtained empirically to provide a relatively small increase in time constant for small inputs, but a much larger increase in time constant for large inputs. For the vergence system, there is an analogous set of elements. In contrast to the adaptation component, the input to the proximal component was represented by a distance stimulus (DS), which drove the perceived distance gain (PDG). The output of PDG was input to both the accommodative proximal gain (APG) and

Table 2. Glossary of acronyms, symbols, and terms

Acronym/Symbol /Term	Definition
ABIAS	Accommodative bias or tonic level; represents the accommodative level in the absence of any accommodative stimulus such as in the dark or empty field.
AC	Accommodative convergence crosslink gain; represents the drive of accommodation on the vergence motor response.
AC/A	Accommodative convergence to accommodation ratio, equal to the slope of the open-loop convergence versus accommodative stimulus (or response) curve.
ACG	Accommodative controller gain; represents the forward loop gain of the accommodative feedback system, with higher gain corresponding to more accurate control.
AD	The deadspace limit value for depth of field; equal to the limit of the idealized deadspace operator representing the objective depth of focus.
ADAPT	Adaptation component which feeds back onto the controller to increase the time constant for decay, so that when the feedback loop is opened, the decay towards the tonic level takes a longer time.
ADD	Plus lens placed before the eyes only for the near-viewing condition; it represents the clinical near add/bifocal prescription.
AE	Accommodative error, or accommodative stimulus minus response; where positive or negative value for AE represents lag and lead, respectively, of the accommodative response.
AE_{rms}	An expression that represents the square root of the sum of all the squared values of AE over the measured time interval divided by the number of time samples. Because it is a squared-value measure, it is insensitive to the sign of AE. However, the sign sensitivity is manifested in the V-shaped curve itself.
APG	Accommodative proximal gain; represents the accommodation system's contribution to the proximal response, which is obtained under open-loop accommodative conditions following closed-loop viewing of the target.
AR	Accommodative response, or change in lens power in response to accommodative stimuli.
AS	Accommodative stimulus, or the dioptric drive for eliciting accommodative response.
CA	Convergence accommodation crosslink gain
CA/C	Convergence accommodation to convergence ratio
D	Diopter, a unit of accommodative stimulus equal to the reciprocal of the distance from the viewing subject in meters.
Depth of Focus (DOF)	The greatest variation in image distance with respect to the retina without appreciable perception of blur. It is represented in the model by the deadspace region for accommodative error, ± AD.
DS	Distance stimulus, which provides perceived distance information for the proximal response
"Induced" Refractive Error (IRE)	The simulated lens placed before the eyes (with distance refractive error fully corrected) at both the specified near *and* far viewing conditions; it represents the optical effect of slowly progressive refractive development caused by nearwork; (-) lens values simulate hyperopic development, whereas (+) lens values simulate myopic development.
MA	Meter angle, a unit of vergence stimulus equal to the reciprocal of the distance from the viewing subject in meters. The interpupillary distance needs to be provided for converting to degrees of visual angle.
Operational Region	The functional region on the V-shaped curve at IRE = 0 D. Operational region being on the left or right half of the V-shaped corresponds to myopigenesis and hyperogenesis, respectively.
PDG	Perceived distance gain, represents the accuracy of perceptual estimate of the distance of a target from the subject.
Panum's fusional Area (PFA)	An area in the retina of one eye, any point of which, when stimulated simultaneously with a single specific point in the retina of the other eye, will give rise to a single fused percept. It is represented in the model by the deadspaced region for vergence error, ± VD.
Refractive Error	The refractive state of the eye at distance with accommodation fully "relaxed", i.e., with zero diopter stimulus to accommodation.
Scleral Tunic	Part of the fibrous tunic (cornea and sclera), or layer of tissue, which serves as a protective covering for the eye.
VBIAS	Vergence bias or tonic level; represents the vergence level in the absence of any vergence stimulus such as in the dark or empty field.
VCG	Vergence controller gain; represents the forward loop gain of the vergence feedback system, with higher gain corresponding to more accurate control.
VD	The limit value for the idealized deadspace operator representing Panum's fusional area.
VE	Vergence error, or vergence stimulus minus response
VR	Vergence response, or change in angle of the lines of sight between the two eye to vergence stimulus.
VPG	Vergence proximal gain; represents the vergence system's contribution to the proximal response, which is obtained under open-loop vergence conditions following closed-loop viewing of the target.
VS	Vergence stimulus, or binocular target change in depth.

Table 3. Summary of model parameter values

Parameter	Parameter values for four refractive groups			
	HYP	EMM	EOM	LOM
Accomm. Deadspace, ± AD (D)	± 0.15	± 0.15	± 0.15	± 0.15
Vergence Deadspace, ± VD (MA)	± 0.012	± 0.012	± 0.012	± 0.012
Accomm Adaptation Gain, K_A	2.0	2.5	4.0	5.5
Vergence Adaptation Gain, K_V	10.0	10.0	10.0	10.0
Perceived Distance Gain, PDG	0.212	0.212	0.212	0.212
Accomm Proximal Gain, APG	2.10	2.10	2.10	2.10
Vergence Proximal Gain, VPG	0.067	0.067	0.067	0.067
Accomm Controller Gain, ACG	21.0	11.5	7.3	6.7
Vergence Controller Gain, VCG	150.0	150.0	150.0	150.0
τ_{A1} (sec)	25	25	25	25
τ_{A2} (sec)	4	4	4	4
τ_{V1} (sec)	50	50	50	50
τ_{V2} (sec)	8	8	8	8
m_A	3	3	3	3
m_V	0.5	0.5	0.5	0.5
Acc. Conv. Gain, AC (MA/D)	0.80	0.80	0.80	0.80
Conv. Acc. Gain, CA (D/MA)	0.37	0.37	0.37	0.37
Tonic Accomm or ABIAS, (D)	1.35	0.80	0.85	0.45
Tonic Vergence or VBIAS, (MA)	0.29	0.29	0.29	0.29

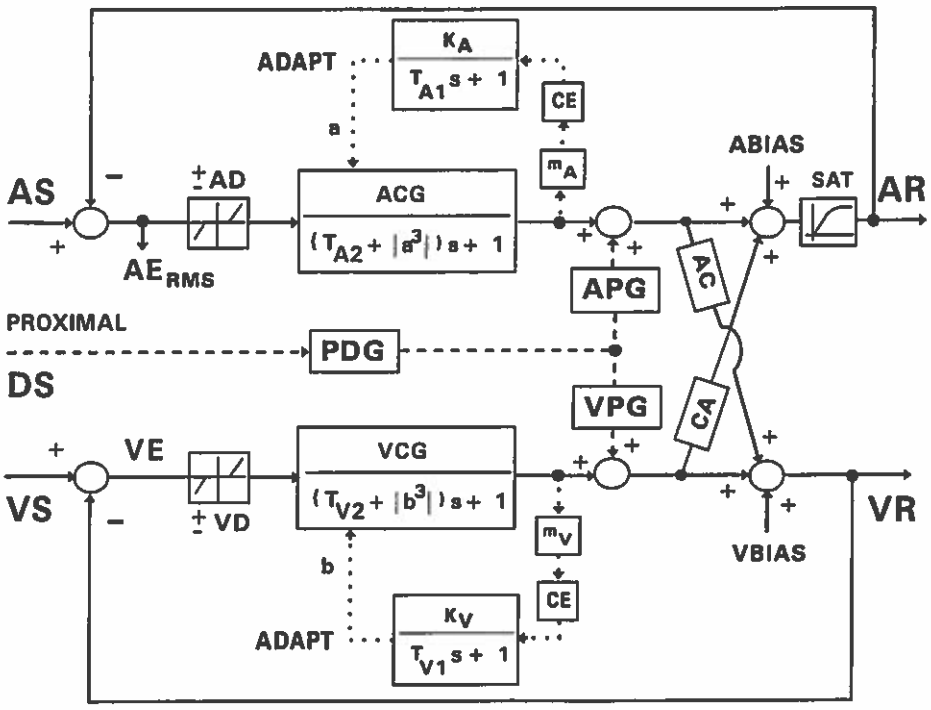

Figure 3. Adaptation model used for nearwork paradigm simulations to obtain parametric relationship between AE_{rms} and IRE (Adapted with permission from Hung & Ciuffreda.[83] See text for details.

vergence proximal gain (VPG) elements, which were summed with the respective controller outputs (Fig. 3).

Dynamic refractive error development model – configuration

The Dynamic Refractive Error Development Model has been described in detail elsewhere,[77] but is summarized briefly below (see Figs. 4A,B). The configuration of the model is based on the interactive dual-feedback model of accommodation and vergence (the latter not shown for simplicity), along with adaptive and proximal components.[77,78,82-84] Added to this basic model is a long-term growth loop that is driven in part by the root-mean square (rms; equal to the average of the absolute value of the instantaneous response over a time interval) of the accommodative error, which simulates retinal defocus that is believed to trigger axial length growth. Due to the squaring process, the directional sign of the blur is potentially lost, although simulations show that during an incremental increase in normal ocular growth[49] or an oculomotor parameter,[77] the blur direction can still be ascertained, as described in the Introduction. Another part of the long-term growth loop is driven by genetic control of the cornea/lens and axial length. The environmental (retinal-defocus induced) and genetically-controlled axial lengths are added together to provide the total axial length. Any mismatch between the power for the cornea/lens and the axial length results in a refractive error. The difference between the accommodative stimulus and the refractive error provides the net accommodative stimulus. For a complete long-term simulation model, the long-term growth loop and the short-term dynamic feedback loop would operate together. For practical computational considerations, however, due to the enormous time difference between the long-term loop (upper loop; time range in 30 years) and short-term feedback loop (lower loop; time range in seconds), a parametric method was needed. In this method, the upper loop was replaced by a parametric relationship between points "a" and "b" in Fig. 4B. For point "a", the refractive error due to the genetic and defocus-induced feedback process was replaced by a selected value for IRE, which served as the stimulus for this relationship. The word "induced" in IRE was used here to represent a selected, rather than feedback-driven, refractive error. To obtain the output "b" of this relationship, a nearwork paradigm was simulated for the (lower) feedback loop of Fig. 4B that consisted of alternating between a 1 hr period of near viewing (3D, 3 MA) and a 5 min period of far viewing (0.25D, 0.25 MA) over 1 work-month (40 hr/wk; 160 hrs total). The steady-state root mean square (rms) of the accommodative error, AE_{rms}, was measured for different selected IRE values to provide the parametric relationship between "b" and "a", respectively. Since the relationship between "b" and "a" should hold for both the upper and lower loops in Fig. 4B, the parametric data for AE_{rms} vs. IRE could then used for the long-term dynamic simulations.

Dynamic refractive error development model simulation

The nearwork paradigm was simulated using an alternating sequence of 1 hr of near viewing (AS = 3D, VS = 3 MA) and 5 min of far viewing (0.25 D, 0.25 MA) for a total of 160 hrs. The AE_{rms} was obtained at the end of the 160 hr trial. The nearwork paradigm was repeated for IRE values ranging from –3.0 to 3.0 D in 0.5 D increments (with the addition of values at 0.25 and 0.75 D to simulate the retinal defocus effects of small, newly-developed refractive error). For each set of IRE values, the near bifocal ADD was varied from 0 to 3 D in 0.5 D increments. These values were input to the model (Fig. 3) by substituting the accommodative stimulus, AS, by AS – IRE – ADD. Simulations were performed under the nearwork paradigm to obtain AE_{rms} for each IRE and ADD value. The combined results were then plotted as AE_{rms} versus IRE for the four refractive groups, with the near bifocal ADD value serving as the parameter for each subplot. Although all other refractive groups showed over-accommodation for far targets[88] per the standard hyperfocal refraction procedure,[89] hyperopes under-accommodated at far because of their initial negative refractive error. Thus, in the simulations, the hyperopic refractive group were constrained to operate only on the lag, or under-accommodation, side of the response for far viewing. This was also done for consistency with earlier nearwork-induced transient myopia (NITM) results.[83,90] In addition, a sensitivity analysis was performed where the parameters were varied at 50, 100, 150 and 200 percent of their nominal values for AC (0.8 MA/D) and CA (0.37 D/MA).

Results

Static nonlinear model

The complete static nonlinear simulation results are plotted as accommodative error versus IRE (Fig. 5A). The signals through the two deadspace operators result in 4 steady-state solutions, representing the 4 possible combinations of operation on either the lead or lag side of the depth-of-focus, and either the eso or exo fixation-disparity side of Panum's fusional area[82]. There are actually two sets of paired solutions (see Table 4 at the end of the Appendix), which are not discernable in Fig. 5A. This is because the separation between each pair is extremely small, since it depends on the Panum's fusinal area (PFA), which is represented in the model by the vergence deadspace ± VD = ± 0.012 MA (see Fig. 3)[91]. Hence the solution pairs (corresponding to conditions 1 and 3, and 2 and 4 in Table 4) are effectively superimposed on each other. In contrast to the solution pairs, the separation between the two sets of solution lines depends on the depth-of-focus (DOF), which is represented by the accommodative deadspace, ± AD = ± 0.15 D (see Fig. 3).[92] The two thin horizontal lines in each subplot represent the limits of the depth-of-focus (DOF). Thus, data within this range are perceived to be clear, and any differences among the curves would not be perceptually distinguishable. Hence,

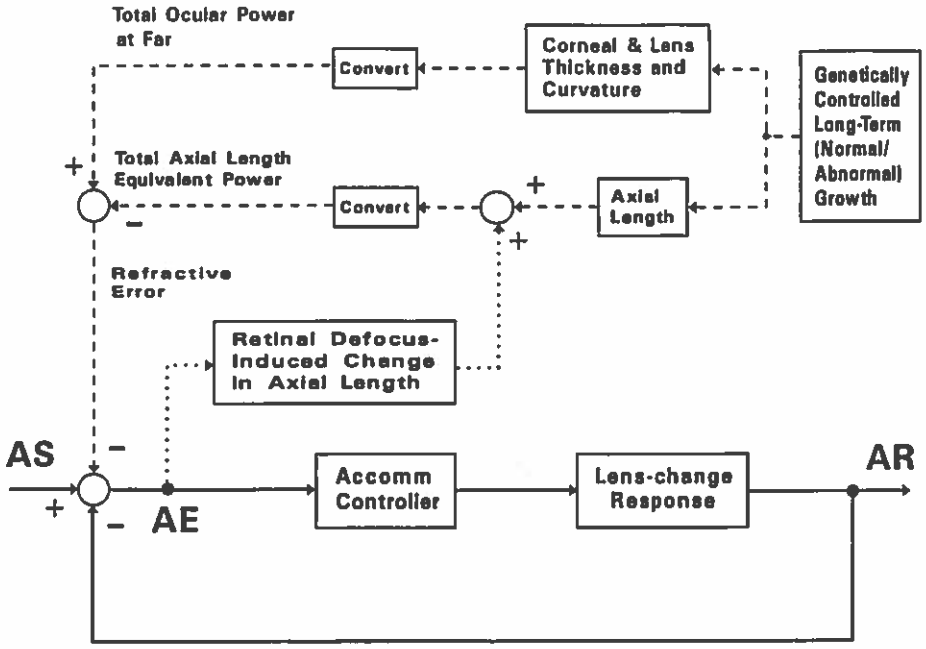

Figure 4. A. Descriptive block diagram of refractive error development model. The basic model (lower loop – solid lines) consists of the conventional accommodative feedback loop where the accommodative error (AE), equal to the accommodative stimulus minus the accommodative response (or AS – AR), is input to the accommodative controller whose output drives the lens to provide the AR. In addition, this model contains signals from the axial length component of the genetically-controlled pathway (upper loop – dashed lines) and the retinal-defocus (AE) induced environmentally-controlled pathway (dotted lines) that sum to provide the total change in axial length. This is converted to total axial length equivalent power and is subtracted from the total ocular power at far (due to combined lens and corneal powers from the refractive component of the genetically-controlled pathway, dashed lines) to provide the overall refractive error. The refractive error is then fed back and added to AS to provide the total accommodative stimulus for driving the lower feedback loop. The upper and lower loops are connected via points "a" (refractive error) and "b" (AE_{rms}) so that they share a common parametric relationship between AE_{rms} and refractive error.

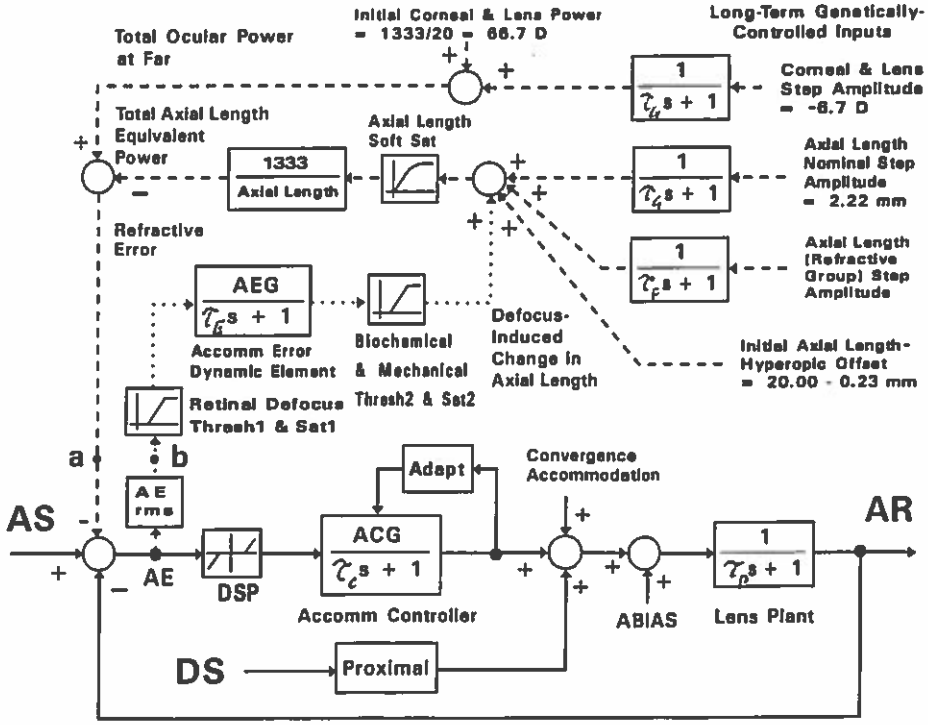

Figure 4. B. Detailed block diagram model of refractive error development model. See text and Hung & Ciuffreda[77] for detailed descriptions.

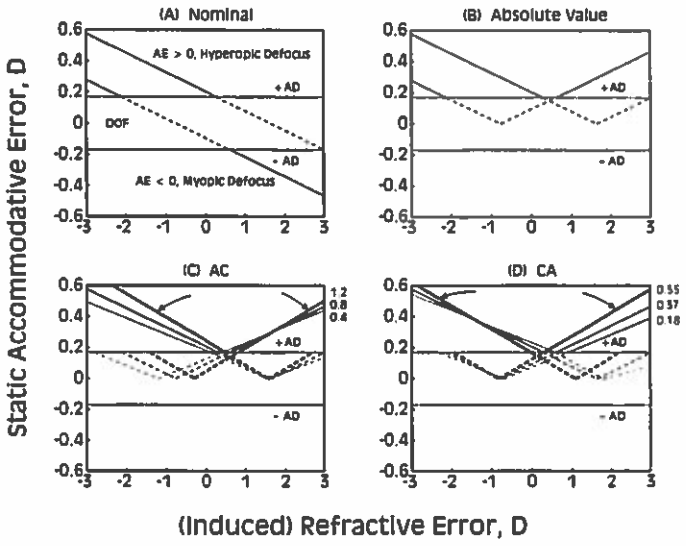

Figure 5. Simulation of static nonlinear model equations showing: (A) nominal static accommodative error, (B) absolute value of static accommodative error, (C) AC variations, and (D) CA variations versus "induced" refractive error (IRE). Note the V shape of the absolute value curves. Region bounded by the horizontal lines designated ± AD represent depth of focus. Solutions within the depth of focus are shown as dashed lines. In the lower subplots, thicker lines are associated with higher parameter values. Arrows in C and D indicate typical corresponding (thickest) lines.

only those portions of the curves outside of this DOF range provide the relevant retinal defocus information. The region above the DOF, where AE > 0, represents the condition of hyperopic defocus, whereas the region below the DOF, where AE < 0, represents the condition of myopic defocus (also see Fig. 1B,C).

Taking the absolute value of the AE data in Fig. 5A results in the plot of Fig. 5B. Note that the myopic defocus curve in Fig. 5A is now seen as the right side of the solid-line V-shaped curve in Fig. 5B. Thus, the sign of retinal defocus is preserved by the negative vs. positive values of the slopes of the solid-line curves in Fig. 5B. That is, the left negative-slope curve represents hyperopic defocus, whereas the right positive-slope curve represents myopic defocus.

The sensitivity plots for variations in AC and CA are shown in Fig. 5 C and D, respectively. It can be seen that the minima of the V-shaped curves (above the DOF region with each curve designated by corresponding-thickness lines; see example curves marked by arrows) shift to the right or left for increased AC or CA values, respectively.

The sign of retinal defocus that was preserved in the V-shaped curve in Fig. 5B can be extracted by means of an incremental increase in IRE (Figs. 6A,B), which represents the equivalent optical power for an incremental increase in normal axial length growth, and would be manifested as a resultant small change in refractive error that evolved slowly in real life but was still uncorrected optically (see Fig. 4B).

Schematic of Differential Effect of Increment in IRE on Axial Growth Rate

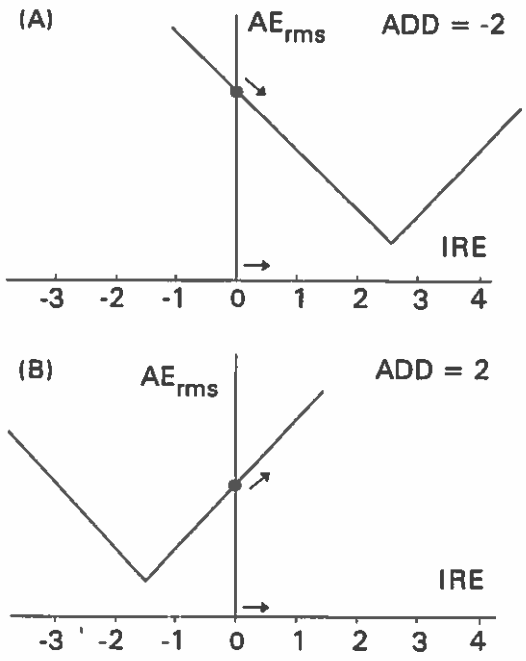

Figure 6. Static schematic analysis for incremental increase in IRE for (A) –2, or (B) +2 D ADD showing decrease or increase in AE, and in turn increase or decrease in axial growth rate, respectively (see Fig. 1 B,C). Assume for simplicity that the initial IRE is at 0 D, representing an emmetropic condition. A) Left branch associated with hyperopic defocus (Fig. 5A); incremental increase in IRE, representing increment in normal axial growth, causes decrease in AErms, and decrease in rate of release of neuromodulators; Results in increase in axial length growth rate (Fig. 1). B) Right branch associated with myopic defocus (Fig. 5A); incremental increase in IRE, representing increment in normal axial growth, causes increase in AErms, and increase in rate of release of neuromodulators; Results in decrease in axial length growth rate (Fig. 1).

This is illustrated schematically for an incremental increase in IRE for ADD = –2 and +2 D in Figs. 6A,B, respectively. Assume for simplicity that normal growth begins at emmetropia, or IRE = 0 D. Therefore, for ADD = –2 D (Fig. 6A), the curve is shifted to the right, so that the operational region (defined here as the functional region on the V-shaped curve at IRE = 0 D) is on the left branch of the V-shaped curve, representing hyperopic defocus (see Fig. 1B). Using the results of our schematic analysis for local retinal growth,[49] we find that such an increase in IRE results in a decrease in AE_{rms} (Fig. 6A), which leads to a decrease in the rate of release of neuromodulators, a decrease in the rate of proteoglycan synthesis, and in turn an increase in axial growth rate. On the other hand, for ADD = +2 D (Fig. 6B), the curve shifts to the left, and the operational region is on the right branch of the V-shaped curve, representing myopic defocus (see Fig. 1C). And analogous to the above, such an incremental increase in IRE results in a decrease in axial growth rate. These

schematic analysis findings are consistent with a resultant relative myopia or hyperopia for the left (hyperopic defocus) or right (myopic defocus) branch, respectively (Figs 1B,C). Thus, the differential effect of an incremental increase in IRE on the two branches in the V-shaped curve provides the information needed to modify appropriately, both the direction and amplitude of axial growth rate. Moreover, these static model findings and their implications on myopigensis and hyperogenesis form the basis for investigating the dynamic refractive error development model.

Dynamic refractive error development model

In each of the dynamic model simulation figures (Figs. 7A–C), the AE_{rms} vs. IRE curves for all the refractive groups (except HYP) are V-shaped, with EMM exhibiting the shallowest slope and LOM the steepest slope. Thus, for a given change in IRE, the resultant retinal defocus is greater for the myopes than for the emmetropes. The HYP curve showed a continued decrease in AE_{rms} with increasing RE. This is primarily because of the constraint for the HYP to operate on the lag side of accommodation for far viewing. Thus, the directional sensitivity of a V-shaped curve is absent in the HYP. Also, in all the plots, there is a shift of the minimum with variation in the parameter values. The minimum shifts to the left for increasing ADD and CA (Figs. 7A and C, respectively), but shifts to the right for decreasing ADD and increasing AC (Fig. 7B). These shifts are consistent with the static nonlinear model simulation results.

For an incremental increase in IRE, and assuming an initial condition of IRE = 0 D, or zero residual refractive error, variation in parameter values can result in an operational region on either the left or right branch of the V-shaped curve, corresponding to development of relative myopia or hyperopia, respectively (see Static Result above (Fig. 6A,B), and Figs 7 A). For example, for ADD = 0 D, the operational region (where IRE ≈ 0) is on the left, or myopigenic, branch. Note that in general infants are hyperopic at birth, and thus this myopic progression would be a natural part of an emmetropization process. However, for ADD = 1 and 2 D, the operational region is on the right, or hyperogenic, branch. Moreover, with an ADD = 0.5 D, the operational region is at a minimum AE_{rms}, which represents a relatively optimal condition that would exhibit neither myopic nor hyperopic development since the potential retinal defocus is minimal.

Discussion

Theories of Myopia development

There are three primary theories of near lens/bifocal therapy related to the prevention and progression of myopia. [1] The "Oculomotor Interactive Theory"[34,92] advocates the use of a near ADD that establishes oculomotor "balance," or "equilibrium," between the accommodative and vergence systems.[34] Based on model and clinical findings, Birnbaum[34] and Schor & Narayan[92] hypothesized that the use of low powered ADDs, such as + 0.50 or + 0.75 D, would result in a "balance" of the interactive accommodative and vergence components as assessed by such clinical measures as the phoria and relative accommodation.[89,93] The low-powered ADDs were proposed to reduce oculomotor "stress", which by a complicated mechanism was believed to prevent and/or reduce the progression of myopia, especially in children. Furthermore, some of these studies suggested that the lens power which produced the optimal effect was both critical and specific. For example, in some children, even slight variation from this optimal nearpoint lens appeared to result in adverse performance.[34] Prescription of low-powered near ADDs in a patient with a high AC/A ratio would act to reduce accommodative drive and thus decrease the amount of accommodative convergence, thereby shifting the person's phoria to a more divergent position (i.e., relatively more exophoric). This is consistent with recent evidence demonstrating that near ADDs are most effective in myopia prevention in children with a high AC/A ratio and near esophoria, with both oculomotor findings appearing to be "risk factors" for myopigenesis.[68,71]

[2] In contrast, the "Biomechanical Theory" (also known as the "Use/Abuse Theory")[94,95] advocates the use of high powered near ADDs in the range of + 1.5 to + 3.0 D. Furthermore, Cohn[94] and Morgan & Munro[95] believed that the process of accommodation per se produces excessive biomechanical stress and strain (i.e., "abuse") on the sclera and contiguous structures, thus causing small but chronic repeated mechanical stretching which slowly and eventually results in axial elongation and myopia. Thus, they believed that minimizing the accommodative response/effort by substantially reducing the blur-driven accommodative response via the high near ADDs would prevent myopia development.[94,95] However, currently there is a lack of support for this notion of biomechanical stress-induced myopia development.[14]

[3] The sensory-based "Retinal Defocus Theory"[20,62,96] advocates the use of a near ADD which minimizes the mean level of retinal defocus, especially at near. In support of this theory, studies in humans have shown that nearwork, which corresponds to increased hyperopic retinal defocus (see Fig. 1), is associated with a higher rate of childhood myopia progression.[14,58,61,69] Moreover, animal studies over the past two decades have clearly demonstrated the myopegenic nature of retinal defocus.[18,21,62] In addition, our schematic model (Fig. 1) has shown that hyperopic defocus during an increment of ocular growth results in a decrease in local blur magnitude, which presumably affects the biochemical processes that alter the local anatomical structure of the sclera and contiguous structures, resulting in axial elongation and myopia.[21] Thus, the introduction of a plus ADD is proposed to counteract this process by reducing the amount of hyperopic retinal defocus, which then inhibits the increased growth process, and thereby reduce the axial growth rate.

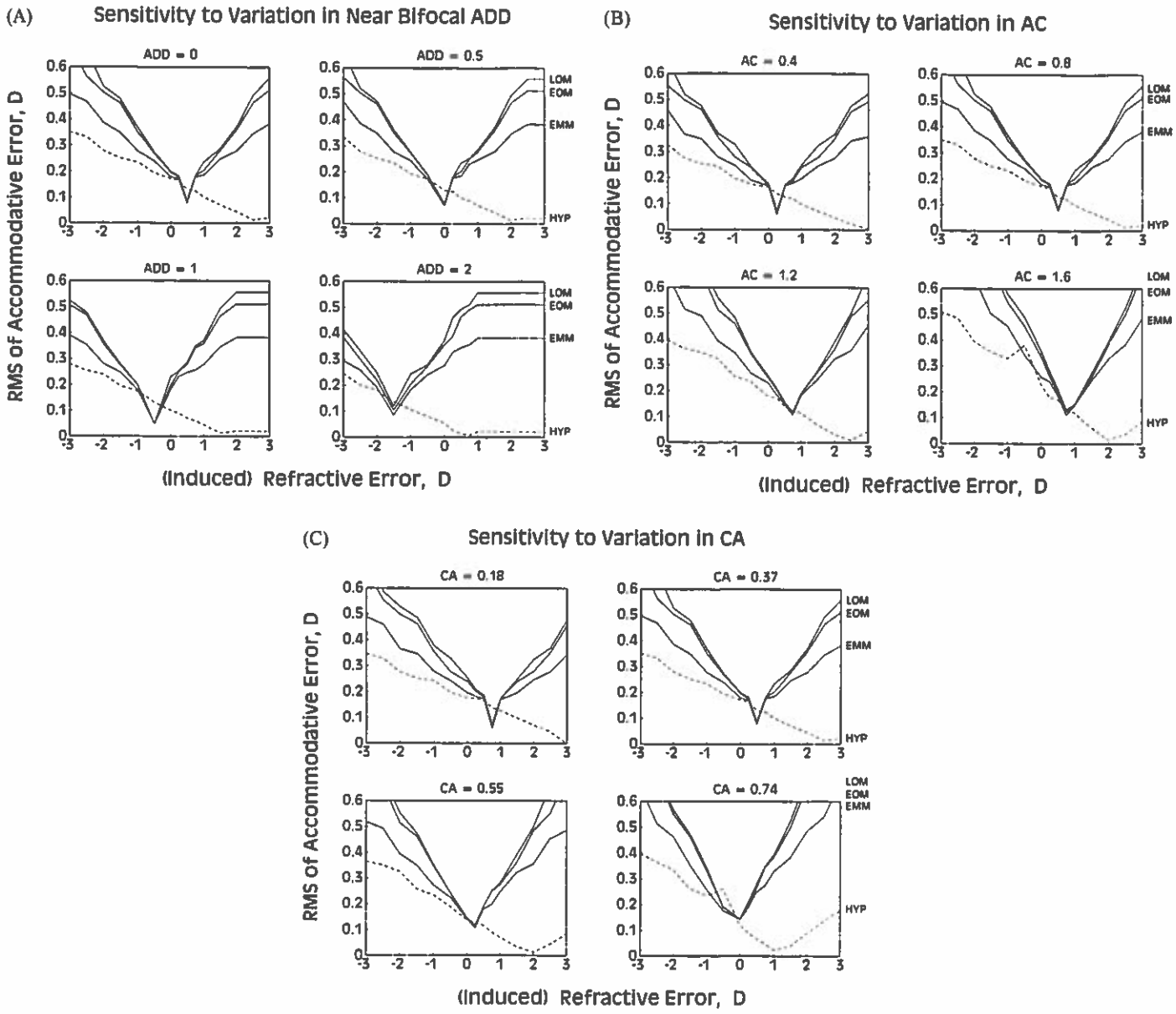

Figure 7. Simulation results of dynamic refractive error development model showing subplots of AE_{rms} vs. IRE for the four refractive groups for variations in (A) ADD, (B) AC, and (C) CA.

Relationship between model and theories

The concept of oculomotor balance as advocated in the "Oculomotor Interactive Theory" is evident in the static model equation (Appendix, Eq. 18). The contributions from the accommodative and vergence stimuli and the various model elements all interact and contribute to the net accommodative error. An imbalance in one or more of these parameters could lead to large errors that may be potentially myopigenic. On the other hand, the introduction of an appropriate ADD (see Eq. 18) could counter such an imbalance to reduce the accommodative error.

Our model does not take into account biomechanical stress-induced effects under the "Biomechanical Theory." However, the theory assumes that the effect of stress is the same under monocular and binocular conditions. Yet, the model equations[77,91] show that the effect of near ADDs on the steady-state accommodative response is substantially different under monocular versus binocular viewing conditions: ADDs in the monocular case simply change the accommodative stimulus level, whereas high ADDs in the binocular case can lead to a conflict in the accommodative and vergence stimuli demands and interactive-based changes in the system's steady-state levels. Thus, the reduction in static accommodation under the normal binocular viewing environment is generally much less than predicted by advocates of the "Biomechanical Theory," whose logic was dictated by monocular expectations. Moreover, our schematic analysis on the V-shaped AE

vs. IRE curve (Fig. 6) showed relatively little effect of high plus bifocal ADDs.

The "Retinal Defocus Theory" is applicable under both monocular or binocular conditions. While Eq. 18 and the subsequent development of the V-shaped curve were derived based on a binocular condition, a similar method can be used to derive both an equation[91] and a V-shaped curve for the monocular condition. Overall, our model equation (Eq. 18) for calculating AE, as well as the logic of our schematic (Figs. 1 and 6) and sensitivity (Figs. 7A–C) analyses, are most consistent with the "Retinal Defocus Theory."

Although our computer-simulation results are most consistent with the "Retinal Defocus Theory," they also provide some support for the "Oculomotor Interactive Theory," but for different reasons. Our model demonstrates that there is a specific "Optimal" ADD, based on the model equations solutions and computer simulations, that shifts the minimum AE_{rms} to occur at IRE equal to zero. In contrast, the "Oculomotor Interactive Theory" suggests that a similar amount of ADD which provides a "balance," or normalization, in clinical oculomotor component values relieves oculomotor "stress," and thereby reduces myopia progression. Thus, with respect to the proposed underlying mechanism, ours is based on sensory processing with a *direct* impact on retinal defocus, whereas the "Oculomotor Interactive Theory" is based on motor control of accommodative and vergence components with an *indirect* impact on retinal defocus, yet both ultimately involve reduced retinal defocus.

Relationship between ADD and myopia

Neetens & Evens[60] varied the ADD based on the amount of myopia (see Table 1). In their bifocal treatment of 8-9 years old children, whose myopia were initially all < 1D, they provided no near correction (i.e., they used plano lens in the lower segment of the bifocal). This meant that the subject's own myopia provided the effective ADD for near reading. On the other hand, during the 10-year follow-up, if the children developed myopia that was 3D or greater, then a near ADD of + 2.5 D (above the far prescription) was provided. Thus, during the early years, when the myopia was just developing, the value of the effective near addition was relatively low. However, in later years, depending on the amount of developed myopia, the effective addition increased but did not exceed + 2.5 D. Overall, Neetens & Evens[60] found that myopia progressed at a faster rate for the single-vision (0.45 D/yr) than bifocal (0.30 D/yr) group, and the difference was significant ($p < .001$). However, since they did not separate the effect of the lower and higher additions, it is unclear from these results whether the benefit obtained for bifocals is due to the early lower effective additions or the later higher + 2.5 D ADDs.

Moreover, under the binocular condition, a high ADD could lead to a conflict between the reduced accommodative demand and the still relatively large vergence demand, which could potentially result in eye strain.[68] Although a recent study[76] found that + 2.00 D ADDs were more effective than + 1.5 D and single-vision lenses, the initial mean myopia for each of their subject population groups was > 3.5 D. High myopes may be more tolerant of such relatively severe binocular conditions and exhibit greater compliance to large ADDs than emmetropes and low myopes.[34] Significantly, the AC/A ratio has been found to be generally higher in myopes than emmetropes in both children and adults.[9,97,98] The higher AC/A ratio could offset in part the reduced accommodative demand due to the near ADD in driving the vergence response, thus maintaining relatively smaller accommodative and vergence errors. Moreover, it has been found that subjects who are esophoric at near benefited the most from bifocal lens wear.[71] Perhaps this relatively greater benefit received by the high myopes could account for the results found.[76]

Refractive error development model

The dynamic refractive error development model simulation results demonstrated how myopigenesis and hyperogenesis could occur (Fig. 7A). It was found that the AE_{rms} vs. IRE relationship was represented by a V-shaped curve (Fig. 7A). This non-monotonic V-shape has considerable significance. For an incremental increase in IRE, the left half of the curve is associated with myopigenesis, whereas the right half is associated with hyperogenesis.[40,41,99,100] Moreover, the value of the IRE at the minimum of the V-shaped curve appears to be *critical* because it determines the transition between myopigenesis and hyperogenesis. This is consistent with the specificity of the near bifocal lens hypothesized under the "Oculomotor Interactive Theory".[34,92]

It would appear at first that developing hyperogenesis could be a means to offset myopic progression. However, in contrast to myopia and its progressive nature,[8,16,32,43,54,101] as well as the refractive changes for relatively large imposed plus and minus lenses in animals during the early growth phase,[13,18,56,65] the refractive condition of hyperopia in many children and young adults exhibits a relative *insusceptibility* to such changes.[40,41,77,99,100] Thus, although it may seem that a large plus ADD would produce hyperogenesis, or at least a reduction in relative myopic progression, its main effect instead appears to be that of simply introducing large retinal defocus, with the intended hyperogenesis having relatively little effect in young human subjects. In contrast, introduction of a large minus ADD results in a large hyperopic retinal defocus (similar to that due to a large lag of accommodation during prolonged nearwork) that would be myopigenic. With this consideration, the optimum value for the control of myopigenesis would therefore be at the point where the accommodative error as well as the induced refractive error are at their minima. This occurs when the minimum of the V-shaped AE_{rms} vs. IRE curve is coincident with IRE = 0.

Such an optimum[102] value could readily be achieved by a shift of the curve using near bifocal ADDs. Such a shift is

predicted by the model equation for accommodative error (see Eq. 18) and can be seen in the model simulation plots (see Fig. 7A). The shift occurs due to the approximate equality of ADD and IRE. For example, a 0.5 D ADD reduces by 0.5 D the amount of IRE needed to achieve the same effect. This is equivalent to shifting the AE_{rms} vs. IRE curve to the left by 0.5 D (see Fig. 7A).

In our recent model of long-term refractive error development, AE_{rms} forms a parametric relationship with IRE that is part of the overall long-term feedback process.[77] Thus, in our present simulations (Fig. 7A–C), it seems desirable to shift the minimum to IRE = 0 D. With both AE_{rms} and IRE at their minimum values, relative refractive stability should be achieved.

The leftward shift of the minimum with increasing ADD (Fig. 7A) provides the intriguing possibility of fine quantitative control of ocular development and emmetropization process. Such a shift incorporates the overall effect of the ADD on oculomotor interactions within the model, including those of the AC/A and CA/C ratios. For example, introducing an ADD = 0.5 D shifts the minimum to IRE = 0 D for our normative model values. This would be consistent with advocacy of low ADDS by the "Oculomotor Interactive Theory" *and* the "Retinal Defocus Theory". In contrast, for an ADD = 2.0 D, the minimum occurs at IRE = – 1.5 D (also see Fig. 6A). Under this latter condition, the minimum would be shifted *further* away from the optimal position. Thus, this would argue against the high ADDs advocated by the "Biomechanical Theory."

The rightward displacement of the minimum for higher AC values (where now IRE = 0 D corresponds to a point on the left half of the V-shaped curve, Fig. 7B) is consistent with clinical and experimental observations that high AC/A ratios and/or near esophoria are related to myopia development.[8] For example, for a high AC value of 1.6 (lower right subplot in Fig. 7B), the minimum has shifted by about 0.8 D to the right, and the operational region is in the relatively far left half of the V-shaped curve, which is associated with myopigenesis.

The leftward displacement of the minimum for higher CA values (where now IRE = 0 D corresponds to a point on the right half of the V-shaped curve, Fig. 7C) is consistent with the finding the bifocals do not appear to control myopia development and progression as well when exophoria at near is present.[8] For example, for a high CA (= 0.74) and no imposed lens (Fig. 7C), the minimum has already shifted to near IRE = 0 D. If a bifocal ADD is introduced, the IRE minimum would be shifted *away from* the optimal position by approximately the same amount as the ADD value, thus resulting in an operational range over the right or hyperogenic half of the V-shaped curve, and as discussed above would have relatively little impact on myopic progression.

Application of model to children

Children and adult oculomotor systems have similar structures and therefore should obey the same physical and physiological principles. The most notable differences are eyeball size and interpupillary distance. Nevertheless, both systems strive to provide clear and single binocular vision. This can be achieved by having negative feedback control of accommodation and vergence, crosslink interactions, as well adaptive properties. Moreover, the parameter values that can be attained in these oculomotor systems are constrained by stability and oculomotor balance considerations.[78] Indeed, sensitivity analysis of oculomotor models have quantified the relatively small range of parameter values to maintain its functional integrity.[103] Therefore, any differences in the model for children and adult are matters of degree rather than of form or configuration. In preliminary investigations, some differences in children and adult parameter values have been observed. For example, Bobier[104] noted in a small group (N = 8) of emmetropic children (mean age = 7.1 years) a mean ACG value of 19.12, which is higher than the nominal adult average value of 10 used in this study. Also, he found a mean CA/C ratio in these emmetropic children of 0.86 D/MA, which is higher than the 0.40 D/MA observed in young adults.[105] In addition, Ciuffreda & Thunyalukul[106] found a larger amount of nearwork-induced transient myopia (NITM) in children (N = 25) (ages 4 to 10 years) than in adults. Although much of the work on model parameter values in children remains preliminary, we are undertaking a series of detailed studies to quantify more of these parameter. Yet, regardless of differences in parameter values, the models for children and adult have the same structure. Therefore, with appropriate parameter adjustments, the present model can be used to simulate oculomotor behavior in children.

Summary

Our simulation of the nearwork model has provided insight into the specific conditions for refractive error development. The critical factor was the finding of a V-shaped AE_{rms} vs. IRE curve, with the position of the minimum being of crucial importance, and where IRE = 0 D represents the optimum value. The ability to control and shift the position of this minimum would provide a potentially powerful means to prescribe specific near bifocal ADDs based on an individual's own model parameter values. This theory needs to be tested by experimental and clinical trials. If the trials are successful, the results could lead to improved worldwide health benefits in reducing the prevalence of myopia.

Acknowledgement

Supported in part by NIH T35 Grant EY07079-14.

References

1. Goldschmidt E. On the etiology of myopia – an epidemiological study. *Acta Ophthalmol.* 1968;98(suppl): 1–72.
2. Sperduto RD, Seigel D, Roberts J, Rowland M. Prevalence of myopia in the United States. *Arch Ophthalmol.* 1983;101:405–407.
3. Lin LLK, Shih YF, Lee YC, Hung PT, Hou PK. Changes in ocular refraction and its components among medical students – a 5-year longitudinal study. *Optom Vis Sci.* 1996;73:495–498.
4. Javitt JC, Chiang YP. The socioeconomic aspects of laser refractive surgery. *Arch. Ophthalmol.* 1994;112: 1526–1530.
5. Mahlman HE. Basic requirements. In: *Handbook of Federal Vision Requirements and Information.* Professional Press, Chicago, IL, USA; 1982:8–18.
6. Diether S, Schaeffel F. Long-term changes in retinal contrast sensitivity in chicks from frosted occluders and drugs: relations to myopia? *Vis Res.* 1999;39:2499–2510.
7. Goss DA. Relation of nearpoint esophoria to the onset and progression of myopia in children. *J Optom Vis Devel.* 1999;30:25–32.
8. Grosvenor T, Goss DA. Etiology of myopia. In: *Clinical Management of Myopia.* Boston, MA: Butterworth-Heinemann; 1999a:49–62.
9. Gwiazda J, Grice K, Thorn F. Response AC/A ratios are elevated in myopic children. *Ophthal Physiol Opt.* 1999;19:173–179.
10. Jiang BC, Morse SE. Oculomotor functions and late-onset myopia. *Ophthal Physiol Opt.* 1999;19:165–172.
11. McBrien NA, Gentle A, Cottriall C. Optical correction of induced axial myopia in the tree shrew: implications for emmetropization. *Optom Vis Sci.* 1999;76: 419–427.
12. Mutti DO, Zaknik K, Adams AJ. Myopia, the nature versus nurture debate goes on. *Invest Ophthal Vis Sci.* 1996;37:952–957.
13. Norton TT. Animal models of myopia: learning how vision controls the size of the eye. *Instit Lab Animal Res Journal.* 1999;40:59–77.
14. Ong E, Ciuffreda KJ. Nearwork-induced transient myopia. In: *Accommodation, Nearwork, and Myopia.* Santa Ana, CA: Optometric Extension Program Foundation, Inc; 1997:97–142.
15. Ong E, Grice K, Held R., Thorn F, Gwiazda J. Effects of spectacle intervention on the progression of myopia in children. *Optom Vis Sci.* 1999;76:363–369.
16. Rosenfield M, Gilmartin B. Myopia and nearwork: causation or merely association? In Rosenfield M, Gilmartin B, eds. *Myopia and Nearwork.* Oxford: Butterworth-Heinemann; 1998:193–206.
17. Shaikh AW, Siegwart JT, Norton TT. Effect of interrupted lens wear on compensation for a minus lens in tree shrew. *Optom Vis Sci.* 1999;76:308–315.
18. Smith EL, Hung LF. The role of optical defocus in regulating refractive development in infant monkeys. *Vis Res.* 1999; 39:1415–1435.
19. Smith EL, Bradley DV, Fernandes A, Boothe RG. Form deprivation myopia in adolescent monkeys. *Optom Vis Sci.* 1999;76:428–432.
20. Wallman J. Can myopia be prevented? In *14th Biennial Research to Prevent Blindness Science Writers Seminar in Ophthalmology.* New York, NY: Research to Prevent Blindness; 1997:50–52.
21. Wildsoet CF. Structural correlates of myopia. In Rosenfield M, Gilmartin B, eds. *Myopia and Nearwork.* Oxford: Butterworth-Heinemann; 1998:32–51.
22. Yackle K, Fitzgerald DE. Emmetropization: and overview. *J Behav Optom.* 1999;19:38–43.
23. Pacella R, McLellan J, Grice K, Del Bono EA, Wiggs JL, Gwiazda JE. Role of genetic factors in the etiology of juvenile-onset myopia based on a longitudinal study of refractive error. *Optom Vis Sci.* 1999;76:381–386.
24. Zadnik K. Myopia development in childhood. *Optom Vis Sci.* 1999;74:603–608.
25. Smith MS. *Evolutionary Genetics.* Oxford: Oxford University Press; 1989:272–303.
26. Kimura T. Developmental change of the optical components in twins. *Acta Soc Ophthalmol Jpn.* 1965;69:963–969.
27. Nakajima A, Kimura T, Kitamura K., et al. Studies on the heritability of some metric traits of the eye and the body. *Jpn J Human Genet.* 1968;13:20–39.
28. Goss DA, Hampton MJ, Wickham MG. Selected review on genetic factors in myopia. *J Am Optom Assoc.* 1988;59:875–884.
29. Sorsby A, Sheridan M, Leary GA. Refraction and its components in twins. *Medical Research Council Special Report Series No. 303.* London: Her Majesty's Stationery Office, 1962.
30. Grosvenor T. Are visual anomalies related to reading ability? *J Am Optom Assoc.* 1977;48:510–516.
31. Baldwin WR. A review of statistical studies of relations between myopia and ethnic, behavioral, and physiological characteristics. *Am J Optom Physiol Opt.* 1981;58:516–527.
32. Curtin BJ. *The Myopias – Basic Science and Clinical Management.* Philadelphia: Harper & Row; 1985.
33. Adams AJ, Baldwin WR, Biederman I, et al. *Myopia: Prevalence and Progression.* Washington, DC: National Academy Press, 1989;1–2,10–22,58–59.
34 Birnbaum MH. *Optometric Management of Nearpoint Vision Disorders*, Boston, MA: Butterworth-Heinemann; 1993:303–309.
35. McBrien NA, Millodot M. The effect of refractive error on the accommodative response gradient. *Ophthal Physiol Opt.* 1986;6:145–149.
36. Hung LF, Crawford MIJ, Smith EL. Spectacle lenses alter growth and refractive status of young monkeys.

Nature Medicine. 1995;1:761–765.
37. Hirsch MJ. Relationship between refraction on entering school and rate of change during the first six years of school: an interim report from the Ojai Longitudinal Study. *Am J Optom Arch Am Acad Optom.* 1962;39:51–59.
38. Hofstetter HW. Some interrelationships of age, refraction, and rate of refractive change. *Am J Optom Arch Am Acad Optom.* 1954:31:161–169.
39. Mantyjarvi MI. Changes of refraction in school children. *Arch Ophthal.* 1985;103:790–792.
40. Erhlich DL, Braddick OJ, Atkinson J, Anker S, Weeks F, Hartley T, Wade J, Rudenski A. Infant emmetropization: longitudinal changes in refractive components from nine to twenty months of age. *Optom Vis Sci* 1997;74:822–843.
41. Gwiazda J, Thorn F, Bauer J, Held R. Emmetropization and the progression of manifest refraction in children followed from infancy to puberty. *Clin Vis Sci.* 1993a;8:337–344.
42. Jiang BC, Woessner WM. Increase in axial length is responsible for late-onset myopia. *Optom Vis Sci.* 1996;73:231–234.
43. Ong E, Ciuffreda KJ. Nearwork-induced transient myopia – a critical review. *Doc Ophthalmol.* 1995;91:57–85.
44. Ciuffreda KJ, Wallis D. Myopes exhibit increased susceptibility to nearwork-induced transient myopia. *Invest. Ophthalmol Vis Sci.* 1998;39:1797–1803.
45. Gwiazda J, Thorn F, Bauer J, Held R. Myopic children show insufficient accommodative response to blur. *Invest Ophthal Vis Sci.* 1993b;34:690–694.
46. Mutti DO and Zaknik K. Is computer use a risk factor for myopia? *J Am Optom Assoc.* 1996;67:521–530.
47. Wu, MM, Edwards, MH. The effect of having myopic parents: an analysis of myopia in three generations. *Optom Vis Sci.* 1999;76:387–392.
48. Saw SM, Chia SE, Chew SJ. Relation between work and myopia in Singapore women. *Optom Vis Sci.* 1999;76:393–396
49. Hung GK, Ciuffreda, KJ. Differential retinal-defocus magnitude during eye growth provides the appropriate direction signal. Submitted.
50. Dowling JE. Retinal processing of vision. In: Greger R, Windhorst U. *Comprehensive Human Physiology: From Cellular Mechanisms to Integration.* Vol. 1, Berlin, Springer-Verlag; 1996:773–778.
51. Windhorst U. Specific networks of the cerebral cortex: functional organization and plasticity. In: Greger R, Windhorst U. *Comprehensive Human Physiology: From Cellular Mechanisms to Integration.* Vol. 1, Berlin, Springer-Verlag; 1996:1105–1136.
52. Rada JA, McFarland AL, Cornuet PK, Hassell JR. Proteoglycan synthesis by scleral chondrocytes is modulated by a vision dependent mechanism. *Curr Eye Res.* 1992;11:767–782.
53. Norton TT, Rada JA. Reduced extracellular matrix in mammalian sclera with induced myopia. *Vis Res.* 1995;35:1271–1281.
54. Christiansen AM, Wallman J. Evidence that increased scleral growth underlies visual deprivation myopia in chicks. *Invest Ophthal Vis Sci.* 1991;32:2134–2150.
55. Marzani D, Wallman J. Growth of the two layers of the chick sclera is modulated reciprocally by visual conditions. *Invest Opthal Vis Sci.* 1997;38:1726–1739.
56. Siegwart JT Jr, Norton TT. Regulation of the mechanical properties of tree shrew sclera by the visual environment. *Vis Res.* 1999;39:387–407.
57. Ficarra, AP, Martino SA, Murray DE, Velasco JL. The effects of bifocals on the progression of childhood myopia. *J Optom Vis Develop.* 1999; 30:21–24.
58. Grosvenor T, Goss DA. Control with added plus power for near work. In: *Clinical Management of Myopia.* Boston, MA: Butterworth-Heinemann; 1999b:113–128.
59. Jensen H. Myopia progression in young school children: a prospective study of myopia progression and the effect of a trial with bifocal lenses and beta blocker drops. *Acta Ophthalmol.* 1991;69 (suppl 200):1–79.
60. Neetens A, Evens P. The use of bifocals as an alternative in the management of low grade myopia. *Bull Soc Belge Ophthaolmol.* 1985;214:79–85.
61. Parssinen O, Heminki E, Klemetti A. Effect of spectacle use and accommodation on myopia progression: final results of a three-year randomized clinical trial among schoolchildren. *Br J Ophthalmol.* 1989;73:547–551.
62. Wallman J, Gottlieb MD, Rajaram V, Fugate-Wentzek LA. Local retinal regions control local eye growth and myopia. *Science.* 1987;237:73–77.
63. Miles FA, Wallman J. Local ocular compensation for imposed local refractive error. *Vis Res.* 1990;30;339–349.
64. Schaeffel F, Diether S. The growing eye: an autofocus system that works on very poor images. *Vis Res.* 1999;39:1585–1589.
65. Schaeffel F, Troilo D, Wallman J, Howland HC. Developing eyes that lack accommodation grow to compensate for imposed defocus. *Vis Neurosci.* 1990;4:177–183
66. Troilo D, Gottlieb, MD, Wallman J. Visual deprivation causes myopia in chicks with optic nerve section. *Curr Eye Res.* 1987;6:993–999.
67. Schwartz JT. Results of a monzygotic co-twin control study of a treatment for myopia. In: *Twin Research 3: Epidemiological and Clinical Studies.* New York, Liss; 1981:249–258.
68. Goss DA. Effect of bifocal lenses on the rate of childhood myopia progression. *Am J Optom Physiol Opt.* 1986;63:135–141.
69. Fulk GW, Cyert LA. Can bifocals slow myopia progression? *J Am Optom Assoc.* 1996;67:749–754.
70. Larrabee PE, Jones, FB. Behavioral effects of low plus lenses. *Percept Mot Skills.* 1980;51:913–914.
71. Goss DA, Grosvenor T. Rates of childhood myopia progression with bifocals as a function of nearpoint phoria: consistency of three studies. *Optom Vis Sci.*

1990;67:637–640.
72. Roberts WL, Banford RD. Evaluation of bifocal correction technique in juvenile myopia. *Optom Weekly.* 1967;58(38) 25–28; 58(39) 21–30; 58(40 23–28; 58(41) 27–34; 58(43): 19–26.
73. Oakley KH, Young FA. Bifocal control of myopia. *Am. J Optom Physiol Opt.* 1975;52:758–764.
74. Grosvenor T, Perrigin DM, Perrigin J, Maslovitz B. Houston Myopia Control Study: A randomized clinical trial. II. Final report by the patient care team. *Am J Optom Physiol Opt.* 1987;64:482–498.
75. Young FA, Leary GA, Grosvenor T. Houston myopia control study: a randomized clinical trial. Part I. Background and design of the study. *Am J Optom Physiol Opt.* 1985;62:605–613.
76. Leung J, Brown B. Progression of myopia in Hong Kong Chinese schoolchildren is slowed by wearing progressive lenses. *Optom Vis Sci.* 1999;76:346–354.
77. Hung GK, Ciuffreda, KJ. Model of refractive error development. *Current Eye Research.* 1999a;19:41–52.
78. Hung GK, Semmlow JL. Static behavior of accommodation and vergence: computer simulation of an interactive dual-feedback system. *IEEE Trans Biomed Engin.* 1980;27:439–447.
79. Panum PL. *Physiologische Untersuchungen Über das sehen mit zwei Augen.* Kiel: Schwersche Buchhandlung, 1858.
80. Hung GK, Ciuffreda KJ, Semmlow JS, Hokoda SC. Model of accommodative behavior in human amblyopia. *IEEE Trans. Biomed Engin.* 1983;30: 665–672.
81. Hung GK, Ciuffreda KJ, Semmlow JS. Modeling of human near response disorders. *Proc. Ninth Annual Northeast Bioengineering Conference.* Rutgers University, New Brunswick, NJ. 1981:192–197.
82. Hung GK. Adaptation model of accommodation and vergence. *Ophthal Physiol Opt.* 1992;12:319–326.
83. Hung GK, Ciuffreda KJ. Adaptation model of near-work-induced transient myopia. *Ophthal Physiol Opt.* 1999b;19:151–158.
84. Hung GK, Ciuffreda KJ, Rosenfield M. Proximal contribution to a linear static model of accommodation and vergence. *Ophthal Physiol Opt.* 1996;16:31–41.
85. Rosenfield M, Ciuffreda, KJ, Hung GK. The linearity of proximally-induced accommodation and vergence. *Invest Ophthal Vis Sci.* 1991;32:2985–2991.
86. Fisher SK, Ciuffreda, KJ, Bird JE. The effect of stimulus duration on tonic accommodation and tonic vergence. *Optom Vis Sci.* 1990; 67:441–449.
87. Rosenfield M, Gilmartin B. Temporal aspects of accommodation. *Optom Vison Sci.* 1989;66:229–234.
88. Ciuffreda KJ, Kenyon RV. Accommodative vergence and accommodation in normals, amblyopes, and strabismics. In: Schor CM, Ciuffreda, KJ. *Vergence Eye Movements: Basic and Clinical Aspects.* Boston, MA: Butterworths; 1983:101–173.
89. Saladin JJ, Phorometry and Stereopsis. In: Benjamin WJ, ed *Borish's Clinical Refraction*, Phil., PA: W. B. Saunders, 1998:724–773.
90. Ciuffreda KJ. Nearwork-induced transient myopia: basic and clinical aspects. *J Optom Vis Dev.* 1999;30:5–20.
91. Hung GK. Quantitative analysis of the accommodative convergence to accommodation ratio: linear and nonlinear static models. *IEEE Trans Biomed Engin.* 1997;44:306–316.
92. Schor CM, Narayan V. Graphical analysis of prism adaptation, convergence accommodation and accommodative convergence. *Am J Optom Physiol Opt.* 1982;59:774–784.
93. Griffin JR, Grisham J. Heterophoria case analysis. In: *Diagnosis and Treatment of Binocular Vision Disorders.* Butterworth-Heinemann, Boston; 1996:63–96.
94. Cohn H. *Untersuchungen der augen von 10,060 schulkindern, nebst vorschlagen zur verbesserung der den augen nachteiligen schulemichtungen.* Leipzig: Verlag von Freidrich Fleischer, 1867. Cited in Goldschmidt E. On the etiology of miopia – an epidemiological study. *Acta Ophthalmol. (Suppl).* 1968; 1–171.
95. Morgan, RW, Munro, M. Refractive problems in northern natives. *Can J Ophthalmol.* 1973;8:226–228.
96. Goss DA, Wickham MG. Retinal-image mediated growth as a mechanism for juvenile onset myopia and for emmetropization. *Doc Ophthalmol.* 1995;90:341–375.
97. Jiang, BC. Parameters of accommodative and vergence systems and the development of late-onset myopia. *Invest Ophthalmol Vis Sci.* 1995;36:1737–1742.
98. Rosenfield M, Gilmartin B. Effect of a near-vision task on the response AC/A of a myope population. *Ophthal Physiol Opt.* 1987;7:225–233.
99. Slataper FJ. Age norms of refraction and vision. *Arch Ophthalmol.* 1950;43;466–481.
100. Rosner J. Hyperopia. In Grosvenor T, Flom MC, eds. *Refractive Anomalies.* Boston, MA: Butterworth-Heinemann; 1991:121–130.
101. Baldwin WR, Adams, AJ, Flattau P, Young-adult myopia. In: Grosvenor T, Flom MC, *Refractive Anomalies – Research and Clinical Applications.* Boston, MA: Butterworth-Heinemann; 1991:104–120.
102. D'Azzo JJ, Houpis CH. *Linear Control System Analysis and Design, Conventional and Modern.* McGraw-Hill, NY; 1988: 542–544.
103. Hung GK, Ciuffreda KJ. Sensitivity analysis of the stimulus-response function of a static nonlinear accommodation model. *IEEE Trans Biomed Engin.* 1998;45: 335–341.
104. Bobier WR. Modelling accommodative lag in myopic children. *Invest Ophthal Vis Sci.* 1999; 40:S449.
105. Rosenfield M, Gilmartin B. Assessment of the CA/C ratio in a myopic population. *Am J Optom Physiol Opt.* 1988;65:168–173.
106. Ciuffreda KJ, Thunyalukul V. Myopic nearwork aftereffects in children. *Invest Ophthal Vis Sci.* 1999;40: S448.

Appendix – Derivation of static nonlinear model equations

The vergence error, VE, is given by

$$VE = VS - VR \tag{1}$$

The output following the vergence controller is

$$V1 = (VE \pm VD) \bullet VCG + VPG \bullet PDG \bullet DS \tag{2}$$

Similarly, the accommodative error, AE, is given by

$$AE = AS - AR \tag{3}$$

The output following the accommodative controller is

$$A1 = (AE \pm AD) \bullet ACG + APG \bullet PDG \bullet DS \tag{4}$$

Also, VR is given by

$$VR = V1 + A1 \bullet AC + VBIAS \tag{5}$$

Substituting Eqs. (2), and (5) into (1) gives

$$VE = VS \quad [\,(VE \pm VD) \bullet VCG + VPG \bullet PDG \bullet DS + A1 \bullet AC + VBIAS\,] \tag{6}$$

Solving for VE gives $VE = \dfrac{VS \mp (VD \bullet VCG) - VPG \bullet PDG \bullet DS - A1 \bullet AC - VBIAS}{1 + VCG}$ (7)

Similarly to above, it can be seen that

$$AR = A1 + V1 \bullet CA + ABIAS \tag{8}$$

Substituting (8) into (3) gives

$$AE = AS \quad AR = AS \quad (A1 + V1 \bullet CA + ABIAS) \tag{9}$$

Substituting (2) into (9) gives

$$AE = AS - \{\, A1 + [(VE \pm VD) \bullet VCG + VPG \bullet PDG \bullet DS] \bullet CA + ABIAS \,\} \tag{10}$$

Substituting (7) into (10) gives

$$AE = AS - \left\{ A1 + \left\{ \left\{ \left[\frac{VS + (VD \bullet VCG) - VPG \bullet PDG \bullet DS - A1 \bullet AC - VBIAS}{1 + VCG} \pm VD \right] \bullet VCG \right\} + VPG \bullet PDG \bullet DS \right\} \bullet CA + ABIAS \right\} \tag{11}$$

Selecting the terms containing A1 and regrouping, we obtain

$$AE = AS - \left\{ \left(1 - \frac{AC \bullet VCG \bullet CA}{1+ VCG}\right) \bullet A1 + \left\{ \left[\frac{VS \mp (VD \bullet VCG) - VPG \bullet PDG \bullet DS - VBIAS}{1+ VCG} \pm VD \right] \bullet VCG + VPG \bullet PDG \bullet DS \right\} \bullet CA + ABIAS \right\} \tag{12}$$

Substituting (4) into (12) gives

$$AE = AS - \left\{ \left(\frac{1+ VCG - AC \bullet VCG \bullet CA}{1+ VCG}\right) \bullet [(AE \pm AD) \bullet ACG + APG \bullet PDG \bullet DS] + \left\{ \left[\frac{VS \mp (VD \bullet VCG) - VPG \bullet PDG \bullet DS - VBIAS}{1+ VCG} \pm VD \right] \bullet VCG + VPG \bullet PDG \bullet DS \right\} \bullet CA + ABIAS \right\} \tag{13}$$

Selecting terms containing AE gives

$$\left(\frac{(1+ ACG) \bullet (1+ VCG) - ACG \bullet VCG \bullet AC \bullet CA}{1+VCG}\right) \bullet AE = AS - \left\{ \left(\frac{1+ VCG - AC \bullet VCG \bullet CA}{1+ VCG}\right) \bullet [(\pm AD) \bullet ACG + APG \bullet PDG \bullet DS] + \left\{ \left[\frac{VS \mp (VD \bullet VCG) - VPG \bullet PDG \bullet DS - VBIAS}{1+ VCG} \pm VD \right] \bullet VCG + VPG \bullet PDG \bullet DS \right\} \bullet CA + ABIAS \right\} \tag{14}$$

Combining term containing AE gives

$$\left(\frac{(1+ ACG) \bullet (1+ VCG) - ACG \bullet VCG \bullet AC \bullet CA}{1+VCG}\right) \bullet AE = AS - \left\{ \left(\frac{- AC \bullet VCG \bullet CA \bullet [(\pm AD) \bullet ACG + APG \bullet PDG \bullet DS]}{1+ VCG}\right) \pm AD \bullet ACG + APG \bullet PDG \bullet DS + \left[\frac{VS \mp (VD \bullet VCG) - VPG \bullet PDG \bullet DS - VBIAS}{1+ VCG} \right] \bullet VCG \bullet CA \pm VD \bullet VCG \bullet CA + VPG \bullet PDG \bullet DS \bullet CA + ABIAS \right\} \tag{15}$$

Rearranging terms gives

$$\left(+ \text{ACG} \bullet \frac{1 + \text{VCG} - \text{AC} \bullet \text{VCG} \bullet \text{CA}}{1 + \text{VCG}} \right) \bullet \text{AE} = \text{AS} - \left\{ \begin{array}{l} \left(\frac{1 + \text{VCG} - \text{AC} \bullet \text{VCG} \bullet \text{CA}}{1 + \text{VCG}} \right) \bullet [(\text{AE} \pm \text{AD}) \bullet \text{ACG} + \text{APG} \bullet \text{PDG} \bullet \text{DS}] + \\ \left\{ \left[\frac{\text{VS} \mp (\text{VD} \bullet \text{VCG}) - \text{VPG} \bullet \text{PDG} \bullet \text{DS} - \text{VBIAS}}{1 + \text{VCG}} \pm \text{VD} \right] \bullet \text{VCG} + \text{VPG} \bullet \text{PDG} \bullet \text{DS} \right\} \\ \bullet \text{CA} + \text{ABIAS} \end{array} \right\} \tag{16}$$

Solving for AE, we obtain

$$\text{AE} = \frac{\begin{array}{l} (1 + \text{VCG}) \bullet \left[\begin{array}{l} \text{AS} \mp (\text{AD} \bullet \text{ACG}) - (\text{APG} + \text{VPG} \bullet \text{CA}) \bullet \text{PDG} \bullet \text{DS} \\ + \text{VD} \bullet \text{VCG} \bullet \text{CA} - \text{ABIAS} \end{array} \right] \\ - \text{VCG} \bullet \text{CA} \bullet \left[\begin{array}{l} \text{VS} \mp (\text{VD} \bullet \text{VCG}) - (\text{VPG} + \text{APG} \bullet \text{AC}) \bullet \text{PDG} \bullet \text{DS} \\ + \text{AD} \bullet \text{ACG} \bullet \text{AC} - \text{VBIAS} \end{array} \right] \end{array}}{(1 + \text{ACG}) \bullet (1 + \text{VCG}) - \text{ACG} \bullet \text{VCG} \bullet \text{AC} \bullet \text{CA}} \tag{17}$$

If either a near bifocal ADD or induced refractive error (see Table 2) is introduced, then the net stimulus is equal to AS – ADD – IRE (see Eq. 18). Note that a negative optical power provides a positive value for the accommodative stimulus, AS. Thus, for example, for AS = 3 D, IRE = +1D (myopic), and ADD = 0D, the net accommodative stimulus would be equal to (3 – 0 – 1), or 2 D. Moreover, if now ADD = 1D, the net accommodative stimulus would be equal to (3 – 1 – 1), or 1 D.

$$\text{AE} = \frac{\begin{array}{l} (1 + \text{VCG}) \bullet \left[\begin{array}{l} \text{AS} - \text{IRE} - \text{ADD} \mp (\text{AD} \bullet \text{ACG}) - (\text{APG} + \text{VPG} \bullet \text{CA}) \bullet \text{PDG} \bullet \text{DS} \\ + \text{VD} \bullet \text{VCG} \bullet \text{CA} - \text{ABIAS} \end{array} \right] \\ - \text{VCG} \bullet \text{CA} \bullet \left[\begin{array}{l} \text{VS} \mp (\text{VD} \bullet \text{VCG}) - (\text{VPG} + \text{APG} \bullet \text{AC}) \bullet \text{PDG} \bullet \text{DS} \\ + \text{AD} \bullet \text{ACG} \bullet \text{AC} - \text{VBIAS} \end{array} \right] \end{array}}{(1 + \text{ACG}) \bullet (1 + \text{VCG}) - \text{ACG} \bullet \text{VCG} \bullet \text{AC} \bullet \text{CA}} \tag{18}$$

Note that for each set of inputs to Eq. 18, there are four solutions corresponding to the combination of signs of the nonlinear deadspace operators (see Table 4).

Table 4. Four combinations of outputs of deadspace operators (as illustrated in Fig. 2) (AD > 0 and VD > 0)

Combination	Linearized Deadspace Equation		Condition	Interpretation	
				Acc. Resp.	Fix. Disp.
(1)	+	+	AE < –AD, VE < –VD	Lead	Eso
(2)	–	+	AE > AD , VE < –VD	Lag	Eso
(3)	+	–	AE < –AD, VE > VD	Lead	Exo
(4)	–	–	AE > AD, VE > VD	Lag	Exo